



Cite this: *Org. Biomol. Chem.*, 2018, **16**, 7903

## Tetraphenylethylene conjugated *p*-hydroxyphenacyl: fluorescent organic nanoparticles for the release of hydrogen sulfide under visible light with real-time cellular imaging†

C. Parthiban,<sup>a</sup> Pavithra M.,<sup>a</sup> L. Vinod Kumar Reddy,<sup>b</sup> Dwaipayan Sen,<sup>b</sup> Melvin Samuel S.<sup>a</sup> and N. D. Pradeep Singh \*<sup>a</sup>

Hydrogen sulfide (H<sub>2</sub>S) behaves like a two-edged sword, at low concentrations it has beneficial and cytoprotective effects, while at higher concentrations it exhibits toxicity. Hence there is a keen interest in developing light responsive H<sub>2</sub>S donors with a spatio-temporal controlled release. Herein, we report visible light activatable tetraphenylethylene conjugated *p*-hydroxyphenacyl (TPE-*p*HP-H<sub>2</sub>S) nanoparticles for the release of hydrogen sulfide (H<sub>2</sub>S) with a real time monitoring ability. Our newly designed photo-responsive single component organic nanoparticle based H<sub>2</sub>S donor is built by integrating the tetraphenylethylene (TPE) moiety and *p*-hydroxyphenacyl (*p*HP) group so that it can display both aggregation-induced emission (AIE) and excited state intramolecular proton transfer (ESIPT) properties. Aggregation-induced emission enhancement was exhibited by our TPE-*p*HP-H<sub>2</sub>S NP donor, which was then explored for the cellular imaging application. The ESIPT by the *p*HP moiety provided unique advantages to our TPE-*p*HP-H<sub>2</sub>S NP donor which include (i) the excitation wavelength extended to >410 nm (ii) a large Stokes shift (iii) a low inner filter effect and (iv) real-time monitoring of H<sub>2</sub>S release by a simple fluorescent colour change. *In vitro* studies showed that the TPE-*p*HP-H<sub>2</sub>S NP donor presents excellent properties like real-time monitoring, photoregulated H<sub>2</sub>S release and biocompatibility.

Received 27th July 2018,  
Accepted 3rd October 2018

DOI: 10.1039/c8ob01629a

rscl.li/obc

### Introduction

In recent times, substantial research work has been carried out for the development of external stimuli responsive gasotransmitters.<sup>1–5</sup> Among the existing gasotransmitters, hydrogen sulfide (H<sub>2</sub>S) is more significant due to its influence over a wide range of physiological and pathological processes.<sup>6</sup> H<sub>2</sub>S acts as a signaling molecule and mediator of important cellular processes causing several beneficiary effects like anti-inflammatory, antioxidative, vasorelaxant and cytoprotective effects.<sup>7,8</sup> H<sub>2</sub>S is made endogenously in a smaller amount by different mammalian tissues as a protecting factor against many diseases like cardiovascular disease, metabolic syndrome, obesity and neurodegenerative diseases.<sup>9–13</sup> Recent studies have acknowledged that H<sub>2</sub>S is a third gaseous transmitter, in addition to carbon monoxide (CO) and nitric oxide

(NO).<sup>14</sup> Interestingly, studies have shown that the biological effects of H<sub>2</sub>S are dependent on its concentration, at low concentrations it has beneficial and cytoprotective effects, while at higher concentrations it exhibits toxicity.<sup>15</sup> Hence, several H<sub>2</sub>S donors triggered by different stimuli (pH,<sup>16</sup> reaction with glutathione (GSH),<sup>17</sup> esterase-activated release,<sup>18</sup> redox-controlled release,<sup>19</sup> and temperature<sup>20</sup>) have been developed. Among them light induced H<sub>2</sub>S donors have gained considerable attention because of their ability to provide spatio-temporal control over the release.<sup>21–23</sup>

To date, different types of UV light responsive Gasotransmitter Donors (GDs) for the release of H<sub>2</sub>S have been developed.<sup>24–26</sup> But the major limitation of using UV light responsive GDs for the release of H<sub>2</sub>S is the phototoxicity associated with the UV light. Of late, Chakrapani and co-workers described BODIPY-caged thiocarbamate based visible light activated carbonyl sulfide (COS) release.<sup>27</sup> The released COS consequently gets hydrolysed into H<sub>2</sub>S in the presence of carbonic anhydrase (Fig. 1a). The limitation of the abovementioned visible light activated H<sub>2</sub>S donor is its inability to monitor the release of H<sub>2</sub>S in real time. Furthermore, the above visible light activated H<sub>2</sub>S donor needs an external agent (carbonic anhydrase) for the release of H<sub>2</sub>S.<sup>27</sup> Later, our group

<sup>a</sup>Department of Chemistry, Indian Institute of Technology Kharagpur, Kharagpur-721302, West Bengal, India. E-mail: ndpradeep@chem.iitkgp.ernet.in

<sup>b</sup>Centre for Biomaterials, Cellular and Molecular Theranostics, VIT University, Vellore-632014, Tamil Nadu, India

†Electronic supplementary information (ESI) available. See DOI: 10.1039/c8ob01629a

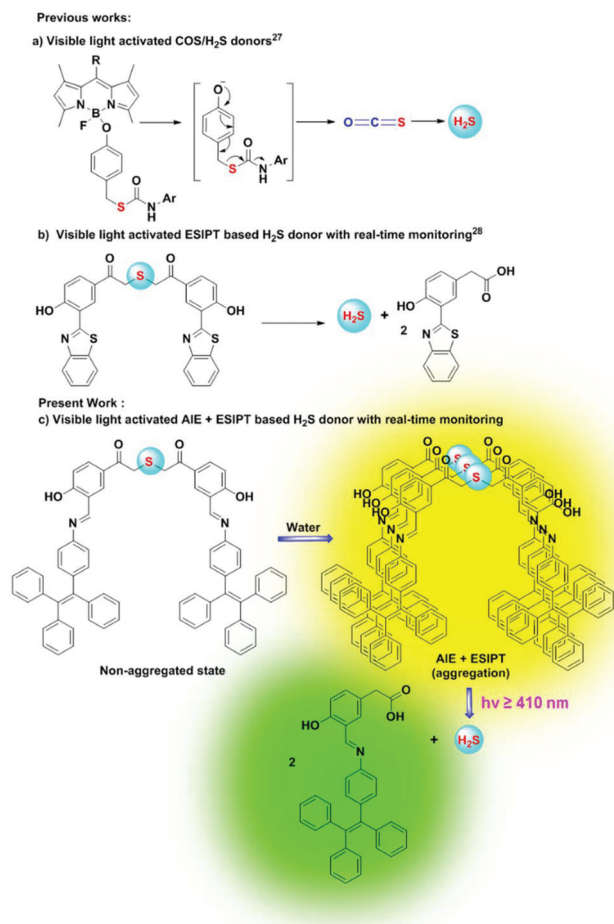


**Fig. 1** Visible light-triggered H<sub>2</sub>S donors, (a) COS/H<sub>2</sub>S donor, (b) ESIPT based H<sub>2</sub>S donor, and (c) design of AIE + ESIPT based photoresponsive single component organic nanoparticles for H<sub>2</sub>S release with a real time monitoring ability.

developed a visible light activated ESIPT based H<sub>2</sub>S donor using *p*-hydroxy phenacyl as a phototrigger with a real time monitoring ability (Fig. 1b).<sup>28</sup>

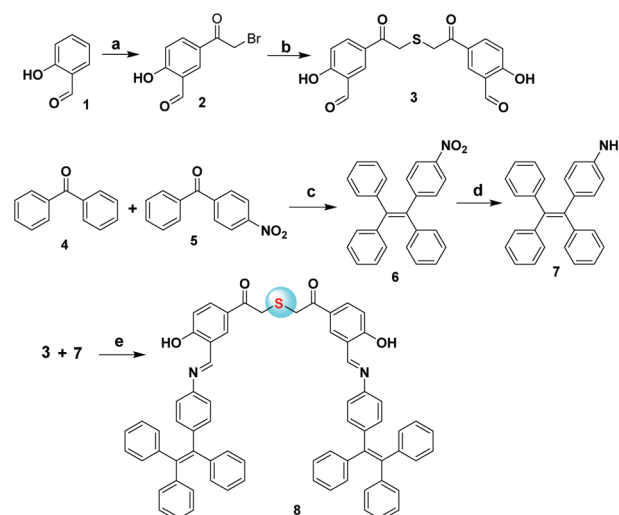
Recently, AIE, a novel photophysical phenomenon, has been utilized in a wide range of applications, such as cell imaging, biosensing and therapeutics, fluorescent sensors, optoelectronic and energy devices *etc.*<sup>29–31</sup> This AIE process has attracted great attention from the scientific community because of its unique properties like high signal to noise ratio, tremendous photostability in the solution phase and remarkable emission properties of a molecule in the aggregated state. AIE chromophores are extremely emissive in their aggregated state however they exhibit weak fluorescence in solution.<sup>30</sup> The regulated intramolecular motion in the aggregated state plays a substantial role. Among the different AIE chromophores, tetraphenylethylene (TPE) has excellent fluorescence in the aggregated state, because of the restriction of molecular motion.<sup>32</sup> TPE has been used in various applications such as chemo/biosensors, solar cells, optoelectronic devices, field effect transistors and light emitting diodes.<sup>33–36</sup>

Keeping the importance of AIE and ESIPT in mind, we intend to design for the first time a photoresponsive single component organic nanoparticle based H<sub>2</sub>S donor which can exhibit the combined benefits of AIE and ESIPT phenomena. The H<sub>2</sub>S donor was developed by integrating the tetraphenylethylene (TPE) moiety and *p*-hydroxyphenacyl (*p*HP) group (Fig. 1c). Our designed H<sub>2</sub>S donor provided advantages like (i) aggregation-induced emission enhancement (ii) a large Stokes shift (iii) the excitation wavelength extended to >410 nm, (iv) unlocking of photorelease of H<sub>2</sub>S in the aggregated state, (v) real-time monitoring of H<sub>2</sub>S release by a simple fluorescent colour change and (vi) no requirement of additional reagent for the release of H<sub>2</sub>S.

## Results and discussion

The TPE-*p*HP-H<sub>2</sub>S donor was synthesized according to the following procedure (Scheme 1). The synthesis of compounds 2 and 3 was carried out according to the reported procedure.<sup>28</sup> On the other hand, compound 4 was treated with 4-nitrobenzophenone (5) in the presence of TiCl<sub>4</sub> in dry THF at reflux for 5 h to afford 6. Next, compound 6 was treated with 10% Pd/C in dry ethanol at reflux for 4 h to furnish 7. Finally, the reaction between 3 and 7 for 3 h in methanol at reflux yields our desired product 8. The products were characterized by NMR (<sup>1</sup>H and <sup>13</sup>C) spectroscopy (Fig. S1 to S5†) and HR-MS (Fig. S6†).

The TPE-*p*HP-H<sub>2</sub>S NP (nanoparticle) donor was prepared by the reprecipitation technique (Scheme S1†). The surface morphology of the TPE-*p*HP-H<sub>2</sub>S NP donor was monitored by high-resolution transmission electron microscopy (HR-TEM). It showed that the prepared nanoparticles were spherical in shape with a size ~35 nm (Fig. 2a). A DLS (dynamic light scat-



**Scheme 1** Synthesis of the TPE-*p*HP-H<sub>2</sub>S donor. Reaction conditions: (a) Bromoacetyl bromide, AlCl<sub>3</sub>, CH<sub>2</sub>Cl<sub>2</sub>, 35 °C, 15 h; (b) Na<sub>2</sub>S·9H<sub>2</sub>O, acetone, H<sub>2</sub>O, 2 h; (c) Zn, TiCl<sub>4</sub>, THF, reflux, 5 h; (d) (NH<sub>2</sub>)<sub>2</sub>-H<sub>2</sub>O, 10% Pd/C, EtOH, reflux; (e) MeOH, reflux, 3 h.

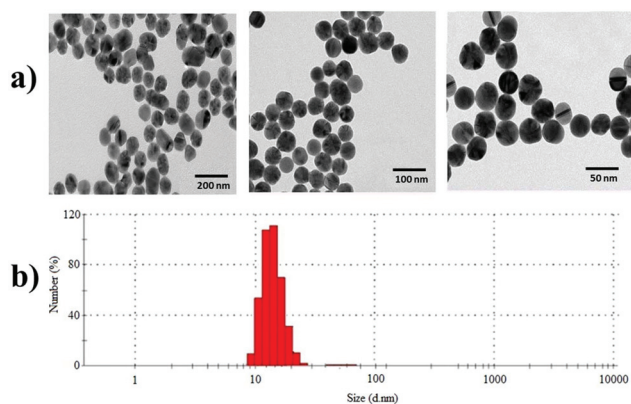


Fig. 2 TPE-*p*HP- $H_2S$  NP donor (a) HR-TEM in aqueous acetonitrile and (b) DLS.

tering) study in Fig. 2b shows that the synthesized nanoparticles have  $\sim 35$  nm of diameter on average, which is almost similar to the size obtained in the HR-TEM image.

The photophysical properties of our newly synthesized  $H_2S$  donor were investigated. The UV spectrum indicated that the TPE-*p*HP- $H_2S$  donor has an absorption band at 372 nm (Fig. 3b). Emission studies were also carried out to understand the ESIPT behavior of the TPE-*p*HP- $H_2S$  donor. In non-hydrogen bonding solvents (chloroform, benzene), only one emission band at  $\lambda_{\max} = 549$  nm (keto form) of the TPE-*p*HP- $H_2S$  donor was noted (Fig. 3a). In non-hydrogen bonding solvents, there is an ultrafast proton transfer occurring from the hydroxyl group of the *p*HP group to the nitrogen atom of the TPE moiety (ESIPT). In addition, in polar aprotic solvents (THF, ACN) and polar protic solvents (MeOH, EtOH), we found two emission bands at  $\lambda_{\max} = 460$  nm (enol form) and  $\lambda_{\max} = 549$  nm (keto form) (Fig. 3c). The new emission at 460 nm (enol form) is due to the existence of a hydrogen bond between the solvent and the hydroxyl group of the TPE-*p*HP- $H_2S$  donor which restricts the ESIPT process. In addition, emission spectra of TPE-*p*HP- $H_2S$  NPs at different concen-

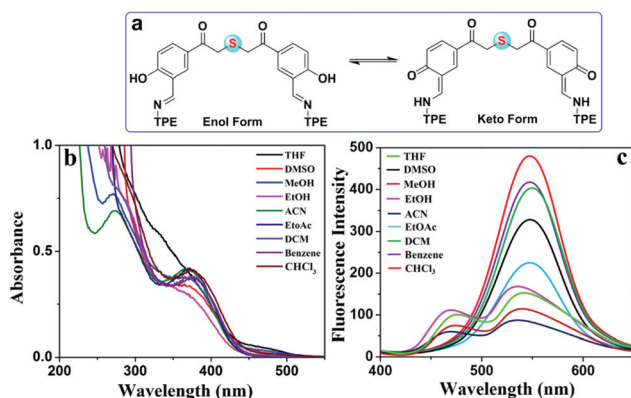


Fig. 3 (a) Keto and enol form of the TPE-*p*HP- $H_2S$  NP donor, (b) UV-Vis absorption spectra and (c) emission spectra of the TPE-*p*HP- $H_2S$  NP donor ( $1 \times 10^{-4}$  M) in various solvents (Ex = 350 nm).

trations in aqueous acetonitrile were recorded and we observed an increase in the emission intensity of TPE-*p*HP- $H_2S$  NPs (Fig. S7†).

To examine the photochemical properties of the TPE-*p*HP- $H_2S$  NP donor, a solution of TPE-*p*HP- $H_2S$  NP donor ( $1 \times 10^{-4}$  M, 5 mL) in  $CH_3CN$ /PBS buffer (0.1 : 9.9 v/v) was irradiated with a medium-pressure mercury lamp (125 W, incident intensity ( $I_0$ ) =  $2.886 \times 10^{16}$  quanta per s) as the source of visible light ( $\lambda \geq 410$  nm) using a suitable UV cut-off filter (1 M  $NaNO_2$  solution) with constant stirring for 20 min. The photodecomposition of the TPE-*p*HP- $H_2S$  NP donor was analyzed by reversed-phase HPLC. As shown in Fig. 4a, the steady disappearance of a peak at  $R_t = 7.42$  min corresponding to the TPE-*p*HP- $H_2S$  NP donor indicates gradual photodecomposition of the  $H_2S$  donor with respect to irradiation time. Furthermore, the appearance and continuous increase in the intensity of the new peak at  $R_t = 4.67$  min indicate the formation of the photoproduct (13). The newly formed peak at  $R_t = 4.67$  was validated as the photoproduct by co-injection and further established by isolation and characterization by  $^1H$  NMR spectroscopy (Fig. S8†). In addition, the time-dependent decomposition of the TPE-*p*HP- $H_2S$  NP donor was found with a first-order rate constant of  $2.76 \times 10^{-4} s^{-1}$  (Fig. 4b).

Furthermore, the photochemical quantum yield ( $\Phi_p$ ) of the TPE-*p*HP- $H_2S$  NP donor was determined as  $0.18 \pm 0.05$  with potassium ferrioxalate as an actinometer. The stability of the TPE-*p*HP- $H_2S$  NP donor was also confirmed under dark conditions in  $CH_3CN$ /PBS containing 10% fetal bovine serum (pH = 7.4) and different pH solutions (pH = 6 and 8) for one week  $\sim 32$  °C. It is clearly shown that the TPE-*p*HP- $H_2S$  NP donor is relatively stable in biological media and in various pH solutions in the dark.

To analyze  $H_2S$  release from the TPE-*p*HP- $H_2S$  NP donor, we utilized the standard methylene blue assay. In this study, a 100  $\mu M$  solution of TPE-*p*HP- $H_2S$  NP donor in pH 7.4 ACN/PBS buffer (0.1 : 9.9) was prepared. Upon irradiation of the TPE-*p*HP- $H_2S$  NP donor, we noted an increase in absorption maximum at 663 nm with increasing irradiation time, validating the ability of the TPE-*p*HP- $H_2S$  NP donor to release  $H_2S$  (Fig. 5a). In addition, we carried out a time-dependent  $H_2S$  generation study; it was observed that the  $H_2S$  generation followed a pseudo-first-order reaction with a rate constant of  $1.22 \times 10^{-7} s^{-1}$ . The concentrations of  $H_2S$  extended a maximum of  $\sim 40$   $\mu M$  in about 20 min and dropped afterward, probably due to volatilization of  $H_2S$  gas (Fig. 5b).

In addition, to demonstrate the  $H_2S$  release only in the presence of light, we observed the release of  $H_2S$  by intermittently switching the visible light source on and off. Fig. 6 shows that on every occasion the light source was switched off,  $H_2S$  release stopped; this evidently specifies that only external stimulus light induces  $H_2S$  release.

With reference to the literature<sup>37,38</sup> and our previous work,<sup>28,39</sup> we proposed a mechanism for the photochemical release of  $H_2S$  from the TPE-*p*HP- $H_2S$  NP donor in aqueous acetonitrile solution as shown in Scheme 2.

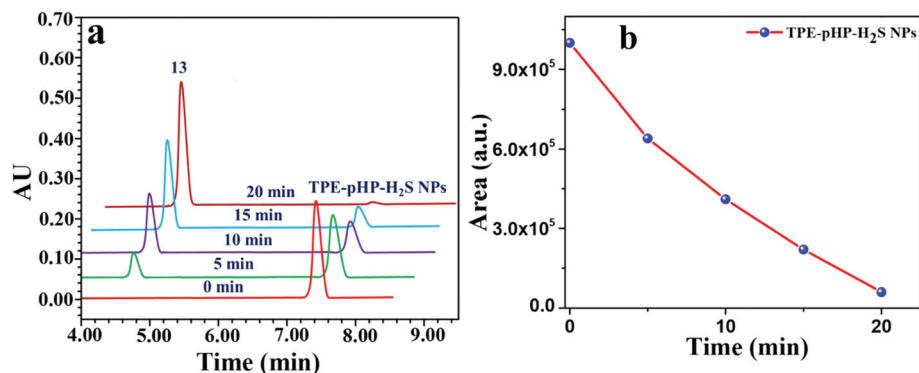


Fig. 4 (a) HPLC profiles of the TPE-*p*HP-H<sub>2</sub>S NP donor at fixed time intervals (0–20 min) of irradiation using visible light ( $\geq 410$  nm) and (b) time course of disappearance of the TPE-*p*HP-H<sub>2</sub>S NP donor was resolved by HPLC analysis.

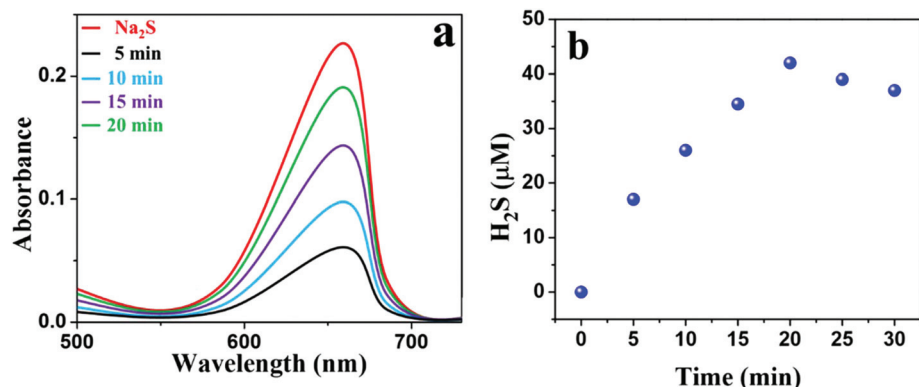


Fig. 5 (a) Spectra of methylene blue assay. Red line: Na<sub>2</sub>S (50 μM). Other lines: H<sub>2</sub>S release from the TPE-*p*HP-H<sub>2</sub>S NP donor upon irradiation at various times and (b) time-dependent H<sub>2</sub>S release of the TPE-*p*HP-H<sub>2</sub>S NP donor was resolved by methylene blue assay and curve fitting found to be pseudo-first-order (rate constant of  $1.22 \times 10^7$  s<sup>-1</sup>).

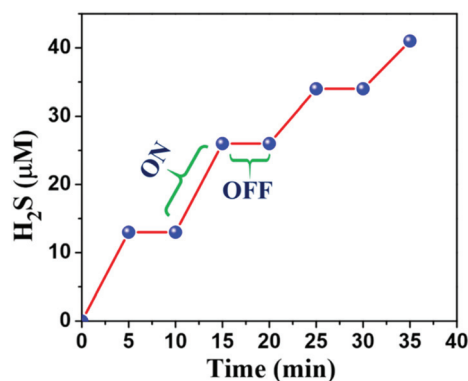


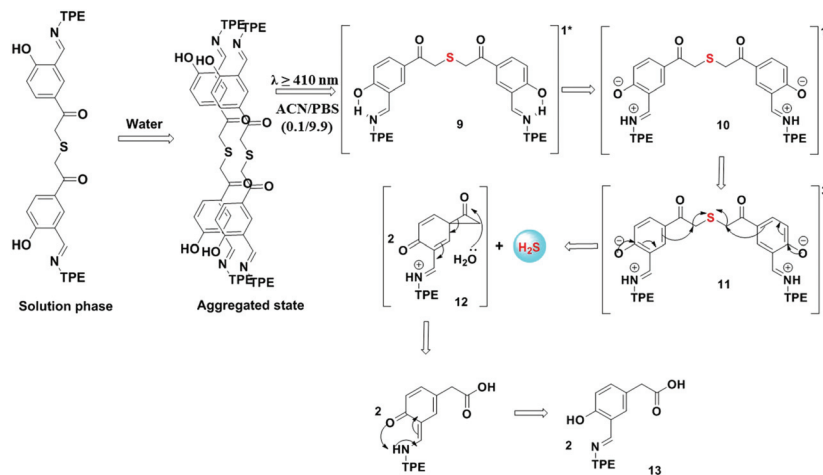
Fig. 6 Progress of the release of H<sub>2</sub>S from the TPE-*p*HP-H<sub>2</sub>S NP donor in bright and dark environments (ON indicates the start of visible light irradiation and OFF indicates the end of visible light irradiation).

At first the aggregation between the molecules (TPE-*p*HP-H<sub>2</sub>S) leads to an inhibition of the intramolecular rotation. Upon irradiation, the TPE-*p*HP-H<sub>2</sub>S NP donor gets excited to its singlet state (S<sub>1</sub>), then it undergoes a rapid ESIP process

from the *p*HP group to the tetraphenyl moiety (9), which results in the deprotonation of the *p*HP group to yield intermediate 10. The zwitterionic intermediate 10 then undergoes intersystem crossing (ISC) to its triplet excited state, from the triplet state it undergoes photo-Favorskii rearrangement to give an assumed spirodiketone 11 with the simultaneous release of the H<sub>2</sub>S. The spirodiketone is then subject to hydrolytic ring opening to yield the photoproduct (13). Moreover, at various pH values the release rate (Table S1<sup>†</sup>) supported the ESIP assistance in the photorelease.

To support the unlocking of photorelease of H<sub>2</sub>S by our donor in the aggregated state, the photolysis of the TPE-*p*HP-H<sub>2</sub>S NP donor was carried out under visible light ( $\geq 410$  nm) in various ACN-H<sub>2</sub>O solvent systems. The ratio of H<sub>2</sub>S release was calculated against different water fractions of ACN (Fig. S10<sup>†</sup>). The photochemical quantum yield progressively increased with increasing  $f_w$  and it was obtained to be the highest at  $f_w = 99$  vol% (Table S2<sup>†</sup>). No considerable H<sub>2</sub>S release was recorded below  $f_w = 80$  vol% and in pure ACN. This proposes that aggregation initiates the H<sub>2</sub>S release process.

Our newly designed H<sub>2</sub>S donor displays a noticeable fluorescence colour change from yellow to green on photoirradiation.



**Scheme 2** Proposed AIE + ESIPT induced H<sub>2</sub>S-releasing mechanism.

tion. At 0 min, the excitation of the TPE-*p*HP-H<sub>2</sub>S NP donor ( $1 \times 10^{-4}$  M, 0.1 : 9.9 ACN/PBS buffer at pH 7.4) at  $\lambda_{\text{max}} = 372$  nm produced only a yellow-emission band at  $\lambda_{\text{max}} = 549$  nm. The steady increase in the irradiation time (0–20 min) results in a continuing decrease in the emission intensity at  $\lambda_{\text{max}} = 549$  nm, with a simultaneous increase in the new emission band at  $\lambda_{\text{max}} = 486$  nm (Fig. 7). The blue shift of the emission suggests the formation of the photoproduct (the blue shift is attributed to the disruption of conjugation from the phenolic hydroxyl group to the carbonyl group). The release of H<sub>2</sub>S from the TPE-*p*HP-H<sub>2</sub>S NP donor was confirmed by fluorescence quenching of coumarin–hemicyanine dye (Scheme S2 and Fig. S11†).

To investigate the cellular uptake and real-time monitoring of H<sub>2</sub>S release from the TPE-*p*HP-H<sub>2</sub>S NP donor within cells, cervical cancer cells HeLa were incubated with the TPE-*p*HP-H<sub>2</sub>S NP donor for 8 h. After incubation, a bright yellow fluorescence (Fig. 8) was produced inside the cells showing good cellular internalization. The co-localization experiments (Fig. S12 and S13†) suggest that the TPE-*p*HP-H<sub>2</sub>S NP donor went selectively into the lysosomes of the HeLa cells. To

demonstrate the real time monitoring capability of the TPE-*p*HP-H<sub>2</sub>S NP donor, confocal microscopy images were obtained at 0, 10 and 20 min of irradiation by visible light respectively. Initially, the cell shows a yellow fluorescence due to aggregation and cellular uptake of **8** (Fig. 8b) and after visible light irradiation for 10 min, we observed a light green fluorescence (Fig. 8c); it shows decomposition of the TPE-*p*HP-H<sub>2</sub>S NPs donor and H<sub>2</sub>S release. After irradiation for 20 min, we observed a complete fluorescence colour change from yellow to green (Fig. 8d), it clearly shows complete photolysis of the TPE-*p*HP-H<sub>2</sub>S NP donor to release H<sub>2</sub>S. Moreover, for the detection of the intracellular H<sub>2</sub>S level we have used coumarin–hemicyanine fluorescence dye (Fig. S14†).

We carried out the cytotoxicity test of the TPE-*p*HP-H<sub>2</sub>S NP donor by using MTT (3-(4,5-dimethylthiazol-2-yl)-2,5-diphenyl-tetrazolium bromide) assay on HeLa cells before and after photolysis (Fig. 9a and b). HeLa cells were incubated with various concentrations of TPE-*p*HP-H<sub>2</sub>S NP donor (1, 5, 10, 15, 20  $\mu\text{m}$ ) for 6 h, and then exposed to photolysis with visible light for 20 min. MTT was added to the cells at 0.4 mg ml<sup>-1</sup> after 72 h of incubation. From the results, we observed that

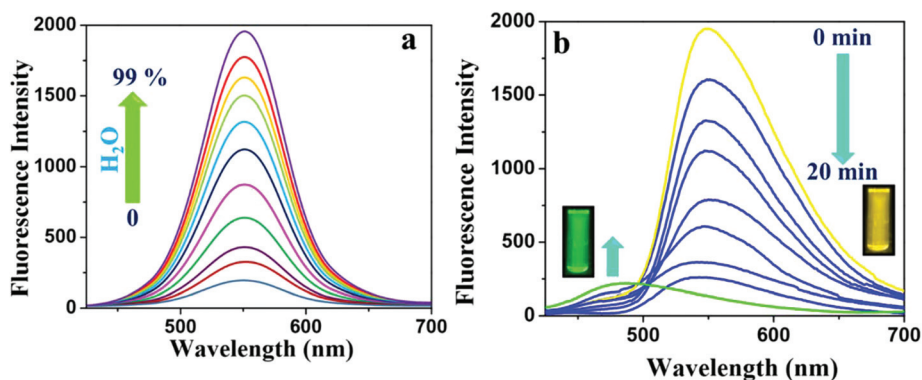


**Fig. 7** (a) Fluorescence response of the TPE-*p*HP-H<sub>2</sub>S NP donor with incremental addition of water (0–99%) and (b) fluorescent spectral change of the TPE-*p*HP-H<sub>2</sub>S NP donor during photolysis at regular intervals of time (0–20 min).

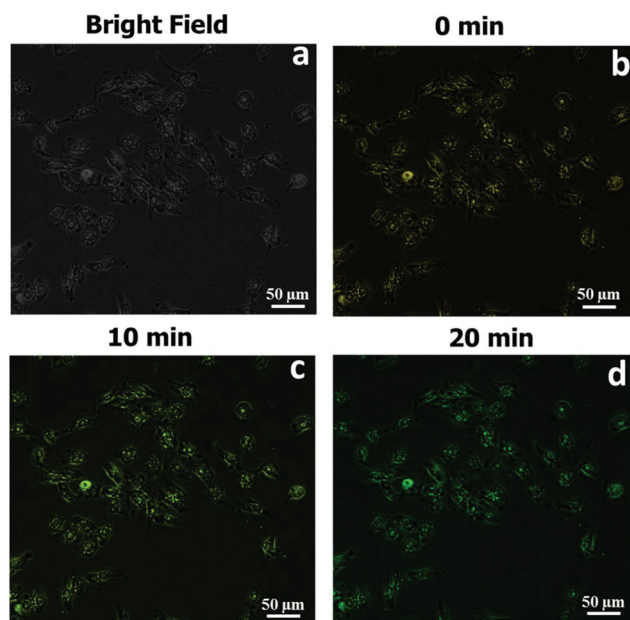


Fig. 8 Confocal microscopy images of internalization of the TPE-*p*HP- $\text{H}_2\text{S}$  NP donor in HeLa cells: (a) bright-field image, (b) 0 min, (c) 10 min and (d) 20 min. Scale bar = 50  $\mu\text{m}$ .

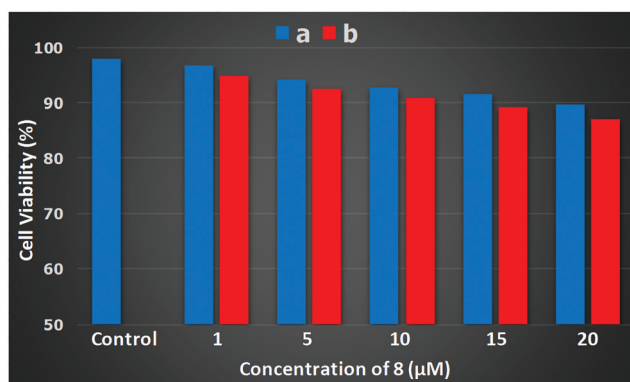


Fig. 9 Cell viability assay of the TPE-*p*HP- $\text{H}_2\text{S}$  NP donor in the HeLa cell line: (a) before and (b) after photolysis for 20 min. Values are depicted as mean  $\pm$  standard deviation from three independent experiments.

there is no confirmation of the inhibition of proliferation of HeLa cells by the TPE-*p*HP- $\text{H}_2\text{S}$  NP donor before and after photolysis, this clearly shows that the  $\text{H}_2\text{S}$  donor TPE-*p*HP- $\text{H}_2\text{S}$  NPs are not cytotoxic at the studied concentration.

## Conclusion

In conclusion, we have demonstrated photoresponsive single component fluorescent organic nanoparticles for  $\text{H}_2\text{S}$  release, utilizing the combined benefits of AIE and ESIPT phenomena with a real time monitoring ability. Our TPE-*p*HP- $\text{H}_2\text{S}$  NP donor exhibited yellow fluorescence and the photorelease

ability was found to be unlocked only in its aggregated state. Upon visible light irradiation, the TPE-*p*HP- $\text{H}_2\text{S}$  NP donor gets excited to its singlet state and then undergoes the ESIPT process to release  $\text{H}_2\text{S}$ . We also demonstrated that our  $\text{H}_2\text{S}$  donor released  $\text{H}_2\text{S}$  in a spatio-temporal controlled manner. Furthermore, we demonstrated the real-time monitoring capability of our  $\text{H}_2\text{S}$  donor at the cellular level with the assistance of a change in fluorescence from yellow to green. Thus, our synthesized TPE-*p*HP- $\text{H}_2\text{S}$  NP donor accomplished the controlled release of  $\text{H}_2\text{S}$  under the visible light without the help of any external agent. In the future, we will focus on developing a near infra-red (NIR) activatable gasotransmitter donor for the release of two different gasotransmitters with a real time monitoring ability.

## Conflicts of interest

There are no conflicts to declare.

## Acknowledgements

We thank DST-SERB (Grant No. EMR/2016/005885) for financial support. DST-FIST for 600 and 400 MHz NMR. C. Parthiban thanks the Science & Engineering Research Board (SERB), New Delhi for N-PDF.

## References

- Z. Xiao, T. Bonnard, A. Shakouri-Motlagh, R. A. L. Wylie, J. Collins, J. White, D. E. Heath, C. E. Hagemeyer and L. A. Connal, *Chem. – Eur. J.*, 2017, **23**, 11294.
- Y. Zhao, H. Wang and M. Xian, *J. Am. Chem. Soc.*, 2011, **133**, 15.
- T. Liu, Z. Xu, D. R. Spring and J. Cui, *Org. Lett.*, 2013, **15**, 2310.
- Y. Wang, G. Zhang, M. Gao, Y. Cai, C. Zhan, Z. Zhao, D. Zhang and B. Z. Tang, *Faraday Discuss.*, 2017, **196**, 9.
- J. Liang, B. Z. Tang and B. Liu, *Chem. Soc. Rev.*, 2015, **44**, 2798.
- C. Zhan, X. You, G. Zhang and D. Zhang, *Chem. Rec.*, 2016, **16**, 2142.
- J. L. Wallace and R. Wang, *Nat. Rev. Drug Discovery*, 2015, **14**, 329.
- D. J. Polhemus and D. J. Lefer, *Circ. Res.*, 2014, **114**, 730.
- B. L. Predmore and D. J. Lefer, *Expert Rev. Clin. Pharmacol.*, 2011, **4**, 83.
- D. J. Polhemus, Z. Li, C. B. Pattillo, G. Gojon, T. Giordano and H. Krum, *Cardiovasc. Ther.*, 2015, **33**, 216.
- S. Mani, A. Untereiner, L. Wu and R. Wang, *Antioxid. Redox Signaling*, 2014, **20**, 805.
- J. Beltowski, G. Wojcicka and A. J. Wisniewska, *Biochem. Pharmacol.*, 2018, **149**, 60.

- 13 B. D. Paul and S. H. Snyder, *Biochem. Pharmacol.*, 2018, **149**, 101.
- 14 W. Zhang, N. Wang, Y. Yu, Y. M. Shan, B. Wang, X. M. Pu and X. Q. Yu, *Chem. – Eur. J.*, 2018, **24**, 4871.
- 15 R. O. Beauchamp, J. S. Bus, J. A. Popp, C. J. Boreiko and D. A. Andjelkovich, *Crit. Rev. Toxicol.*, 1984, **13**, 25.
- 16 J. Kang, Z. Li, C. L. Organ, C. M. Park, C. T. Yang, A. Pacheco, D. Wang, D. J. Lefer and M. Xian, *J. Am. Chem. Soc.*, 2016, **138**, 6336.
- 17 D. Liang, H. Wu, M. W. Wong and D. Huang, *Org. Lett.*, 2015, **17**, 4196.
- 18 Y. Zheng, B. Yu, K. Ji, Z. Pan, V. Chittavong and B. Wang, *Angew. Chem., Int. Ed.*, 2016, **55**, 4514.
- 19 A. Stein and S. M. Bailey, *Redox Biol.*, 2013, **1**, 32.
- 20 Y. Zhao, T. D. Biggs and M. Xian, *Chem. Commun.*, 2014, **50**, 11788.
- 21 P. Stacko, L. Muchova, L. Vitek and P. Klan, *Org. Lett.*, 2018, **20**, 4907.
- 22 M. Popova, T. Soboleva, S. Ayad, A. D. Benning and L. M. Berreau, *J. Am. Chem. Soc.*, 2018, **140**, 9721.
- 23 R. Sakla and A. Jose, *ACS Appl. Mater. Interfaces*, 2018, **10**, 14214.
- 24 N. O. Devarie-Baez, P. E. Bagdon, B. Peng, Y. Zhao, C. M. Park and M. Xian, *Org. Lett.*, 2013, **15**, 2786.
- 25 Y. Zhao, S. G. Bolton and M. D. Pluth, *Org. Lett.*, 2017, **19**, 2278.
- 26 Z. Xiao, T. Bonnard, A. Shakouri-Motlagh, R. A. L. Wylie, J. Collins, J. White, D. E. Heath, C. E. Hagemeyer and L. A. Connal, *Chem. – Eur. J.*, 2017, **23**, 11294.
- 27 A. K. Sharma, M. Nair, P. Chauhan, K. Gupta, D. K. Saini and H. Chakrapani, *Org. Lett.*, 2017, **19**, 4822.
- 28 Y. Venkatesh, J. Das, A. Chaudhuri, A. Karmakar, T. K. Maiti and N. D. Pradeep Singh, *Chem. Commun.*, 2018, **54**, 3106.
- 29 Y. Wang, G. Zhang, M. Gao, Y. Cai, C. Zhan, Z. Zhao, D. Zhang and B. Z. Tang, *Faraday Discuss.*, 2017, **196**, 9.
- 30 J. Liang, B. Z. Tang and B. Liu, *Chem. Soc. Rev.*, 2015, **44**, 2798.
- 31 C. Zhan, X. You, G. Zhang and D. Zhang, *Chem. Rec.*, 2016, **16**, 2142.
- 32 W. Zhang, N. Wang, Y. Yu, Y. M. Shan, B. Wang, X. M. Pu and X. Q. Yu, *Chem. – Eur. J.*, 2018, **24**, 4871.
- 33 H. Zhang, H. Li, J. Wang, J. Sun, A. Qin and B. Z. Tang, *J. Mater. Chem. C*, 2015, **3**, 5162.
- 34 H. T. Feng, S. Song, Y. C. Chen, C. H. Shen and Y. S. Zheng, *J. Mater. Chem. C*, 2014, **2**, 2353.
- 35 Z. Zhao, J. W. Y. Lam and B. Z. Tang, *J. Mater. Chem.*, 2012, **22**, 23726.
- 36 X. Liu, J. Jiao, X. Jiang, J. Li, Y. Cheng and C. Zhu, *J. Mater. Chem. C*, 2013, **1**, 4713.
- 37 X. Luo, J. Wu, T. Lv, Y. Lai, H. Zhang, J. Jian Lu, Y. Zhang and Z. Huang, *Org. Chem. Front.*, 2017, **4**, 2445.
- 38 P. Klan, T. Solomek, C. G. Bochet, A. Blanc, R. Givens, M. Rubina, V. Popik, A. Kostikov and J. Wirz, *Chem. Rev.*, 2013, **113**, 119.
- 39 S. Barman, S. K. Mukhopadhyay, S. Biswas, S. Nandi, M. Gangopadhyay, S. Dey, A. Anoop and N. D. P. Singh, *Angew. Chem., Int. Ed.*, 2016, **128**, 4266.